RNA (1998), *4*:1295–1303. Cambridge University Press. Printed in the USA.

Correlation between bending of the VM region and pathogenicity of different Potato Spindle Tuber Viroid strains

AXEL SCHMITZ and DETLEV RIESNER

Institut für Physikalische Biologie, Heinrich-Heine-Universität Düsseldorf, Universitätsstr. 1, D-40225 Düsseldorf, Germany

ABSTRACT

Only 40 of the 359 nucleotides of Potato Spindle Tuber Viroid (PSTVd) represent the virulence-modulating (VM) region. Minor sequence variations in this domain distinguish mild from severe and even necrotic strains. Our recent hypothesis (Owens RA et al., 1996, *Virology 222*:144–158) that these differences result in varying degrees of bending of this part of the molecule could be tested experimentally. By in vitro transcription and partial double-strand formation, three types of model RNAs were prepared and subjected to electrophoresis in polyacrylamide gels: (1) Fragments representing the VM regions of six different PSTVd strains; (2) control fragments containing a bulge-loop as a rigid bend or an internal loop as a point of increased flexibility; and (3) dsRNAs of 36, 39, and 43 bp as length standards. Migration anomalies in gels of increasing percentage were evaluated and resulted in the following conclusions. In the absence of Mg^{2+}, the VM regions differ only in terms of flexibility. Addition of Mg^{2+} induces conformational changes in these RNAs. All strains but Mild exhibit a rigid bend, and the angle of bending increases monotonically with the pathogenicity of the strain. The data are discussed in terms of a mechanism of pathogenicity, that protein-binding to the VM region is the primary pathogenic event.

Keywords: dsRNA-activated protein kinase (PKR); Mg^{2+}-induced conformational change; native PAGE; RNA–protein interactions; RNA three-dimensional structure

INTRODUCTION

Viroids are single-stranded, circular RNA molecules of 250–600 nt; they are the smallest known pathogens affecting only plants. They do not encode proteins and consequently rely completely on host factors for both replication and transport.

Potato Spindle Tuber Viroid (PSTVd) was the first viroid described (Diener & Raymer, 1967; Diener, 1971) and still is studied in most detail (for reviews, see Riesner & Gross, 1985; Diener, 1987; Semancik, 1987; Symons, 1990). This RNA comprises 359 nucleotides and adopts an unbranched, rodlike secondary structure through intramolecular base pairing (Fig. 2) (Gross et al., 1978). It causes epinasty and stunting in tomato plants. Two to four weeks after inoculation, approximately 20% of all cells are infected, each containing 10^4–10^5 PSTVd molecules that are localized mainly in the nucleoli (Schumacher et al., 1983; Harders et al., 1989). Replication of PSTVd involves RNA polymerase II (Schindler & Mühlbach, 1992) transcribing the circular molecule via a rolling circle mechanism into an oligomeric (−)-strand, which then serves as a template for the synthesis of a (+)-oligomer (Branch & Robertson, 1984). This assumes a complex processing structure, which is recognized by not yet identified cellular factors, cleaved, and ligated to the progeny (+)-circle (Baumstark et al., 1997).

In comparison to the viroids replication, much less is understood about its pathogenic action. Figure 1 illustrates the wide range of symptom severity caused by different strains of PSTVd. Because the viroid does not encode proteins, a direct interaction of the (−)- or (+)-strand RNA with cellular factors must be the cause for the pathogenic response of the host plant. Strain variation is the result of minor sequence differences that are localized in two nonadjacent stretches of the viroid RNA. These stretches are partially base paired with each other in the rod-like native structure of circular (+)-PSTVd (Fig. 2), thereby forming the so-called virulence-modulating (VM) region. The VM region is one of five domains that can be distinguished in PSTVd

Reprint requests to: Detlev Riesner, Institut für Physikalische Biologie, Heinrich-Heine-Universität Düsseldorf, Universitätsstraße 1, 40225 Düsseldorf, Germany; e-mail: riesner@biophys.uni-duesseldorf.de.

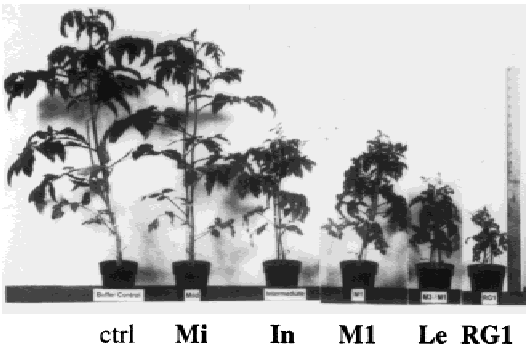

FIGURE 1. Pathogenicity of various PSTVd strains. Symptoms of PSTVd infection in Rutgers tomato approximately 7 weeks after inoculation with PSTVd RNA: Mi, Mild; In, Intermediate; M1, M1; Le, Lethal; RG1, RG1; ctrl, buffer control (non-infected). PSTVd strain Severe was not tested in this assay. Figure is modified from Owens et al. (1996).

based on sequence comparisons with related viroids (Keese & Symons, 1985) (Fig. 2). Schnölzer et al. (1985) evaluated the thermodynamic stabilities of the VM regions of four different PSTVd strains and found the stability inversely related to the pathogenicity of the respective variant. Such an explanation appeared attractive because thermodynamic instability would facilitate the putative interaction of the viroid with cellular RNAs. Later it was observed that more severe variants outcompete milder ones when present in the same plant, but no big difference in growth kinetics was observed when these were propagated on separate individuals (Gruner et al., 1995). It was suggested and supported experimentally that mutations in the VM region might affect the stability of the whole molecule and the rodlike structure might switch easier to an alternative, metastable structure in the severe strains. If this alternative structure had an implication for both pathogenicity and replication, a severe strain could overgrow a milder one by more efficiently recruiting limiting cellular factors, e.g., RNA polymerase II. Both of these previous studies, however, were restricted to only four to six different strains. Inclusion of more variants showed that neither the stability of the VM region nor that of the whole molecule correlated with the pathogenicity consistently for all viroid strains tested (Owens et al., 1996). Instead, a structural model for pathogenicity was proposed, assuming that the native structure of (+)-PSTVd is essential for the pathogenic action. On the basis of the thermodynamically optimal base pairing schemes and taking into account the asymmetric distribution of nucleotides in loops, an increase in bending of the VM regions from intermediate (straight) to severe strains and even more to necrotic strains was suggested. In the mild strains, bending appeared to be in the opposite direction.

In the present work, we tested this hypothesis by probing experimentally the three-dimensional structure of the VM regions belonging to six different PSTVd strains. For this purpose, short RNA duplexes representing the VM regions were subjected to native polyacrylamide gel electrophoresis and their mobilities in the gel were compared with those of completely base paired RNA fragments of the same respective molecular weight. Comparison with model RNAs containing either a flexible internal loop or a rigidly bent bulge-loop allowed us to discriminate between static bending and isotropic flexibility of the fragments under study. Our results mainly support our hypothesis reported earlier (Owens et al., 1996) and elucidate some features in more detail. The correlation between pathogenicity and bending of the VM region holds only in the presence of Mg^{2+}, whereas, without Mg^{2+}, all VM regions reflect the behavior of flexible internal loops. We propose that the observed differences in VM-region bending might be of relevance for the affinity of a host protein to the viroid and that the strength of this interaction determines the pathogenic response of the infected plant.

RESULTS

Reference RNAs allow for the discrimination between bending and flexibility

Native PAGE was employed for the detection of differences in the structure of strain-specific VM regions. Unbranched nucleic acid structures exhibit reduced electrophoretic mobility if they contain points of rigid bending or increased flexibility. While the migration anomaly of flexible structures is small and remains more or less constant regardless of gel concentration, i.e., pore size, rigidly bent species show more pronounced retardation that increases when the pore size of the gel is reduced (Bhattacharyya & Lilley, 1989; Kahn et al., 1994; Zacharias & Hagerman, 1995).

To test whether this holds true even for fragments of the small size of this study, we constructed an RNA duplex with a centrally located A_2-bulge loop (bL in Fig. 2) and another with an A_4-internal loop (iLA in Fig. 2). As with the VM-region RNA hybrids, these resulted from the annealing of short RNA strands transcribed in vitro from DNA templates. Bulge-loops introduce static bends whose size depends on the number of loop nucleotides, whereas internal loops represent points of increased isotropic flexibility (Zacharias & Hagerman, 1995, 1996). The migration anomaly is expressed by the *k*-value, which is the ratio of the apparent size to the real size of an RNA duplex, where the apparent size is determined by comparison with fully base paired fragments of 36, 39, and 43 base pairs. Thus, the *k*-value is larger for a more retarded RNA. The RNA standards were also annealed from complementary in vitro transcripts (Fig. 2).

As can be seen in Figure 3, the two structures displayed the expected dependencies of migration anom-

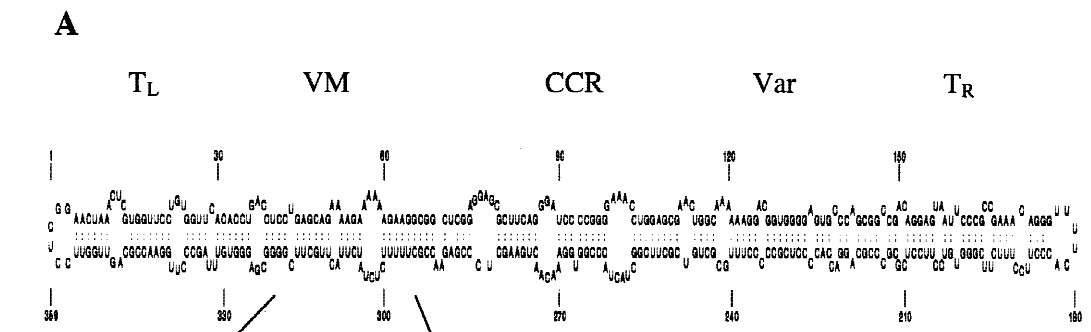


```
                U                  AAA A
5′GGCGCCGC  GAGCAGA—AAAGA        AGAGGCCGGCC3′
3′CCGCGGCG  UUCGUUU  UUUCU        UUUCCGGCCGG5′
                C        C         AUCUC
```

Mild: $A_{310} \rightarrow U$, $+U_{311a}$

```
                43                 58
                U          AA      AAAA
5′GGCGCCGC  GAGCAG    AAGA        AGAGGCCGGCC3′
3′CCGCGGCG  UUCGUU    UUCU        UUUCCGGCCGG5′
                313      308       298
                C          CA      AUCUC
                318                303
```

Intermediate

```
                  A        AA       AAAA
5′GGCGCCGCUG    CAAG    AAGA        AGAGGCCGGCC3′
3′CCGCGGCGGC    GUUC    UUCU        UUUCCGGCCGG5′
                UUC        A        AUCUC
```

M1.1: $G_{46} \rightarrow C$, $C_{47} \rightarrow A$

```
                U          AA       AAAA
5′GGCGCCGC  GA—CAAG    AAGA        AGAGGCCGGCC3′
3′CCGCGGCG  UU  GUUC    UUCU        UUUCCGGCCGG5′
                C  C       A        AUCUC
```

M1.3: $G_{46} \rightarrow C$, $C_{47} \rightarrow A$

```
                U          AA       AAAA
5′GGCGCCGC  GAGCAGA    AAGA        AGAGGCCGGCC3′
3′CCGCGGCG  UUCGUUU    UUCU        UUUCCGGCCGG5′
                C        C*        AUCUC
```

Severe: $+A_{50a}$, $+U_{311a}$, $-A_{310}$

```
                U          AA       AAAA
5′GGCGCCGC  GACAAG     AAGA        AGAGGCCGGCC3′
3′CCGCGGCG  UUGUUC     UUCU        UUUCCGGCCGG5′
                CC         A        AUCUC
```

Lethal: $G_{46} \rightarrow C$, $C_{47} \rightarrow A$, $C_{315} \rightarrow U$, $U_{317} \rightarrow C$

```
                  A        AA       AAAA
5′GGCGCCGCUG    CAAG    AAGA        AGAGGCCGGCC3′
3′CCGCGGCGGC    GUUC    UUCU        UUUCCGGCCGG5′
                CUC        A        AUCUC
```

RG1: $G_{46} \rightarrow C$, $C_{47} \rightarrow A$, $U_{317} \rightarrow C$

```
                        AAAA
5′GGCGCCGCUAGACUUGC     GCCUAUUAGUGGCCGGCC3′
3′CCGCGGCGAUCUGAACG     CGGAUAAUCACCGGCCGG5′
                        AAAA
```

iLA

```
                        AA
5′GGCGCCGCUAGACUUGCC    CGUAUCACGUGGCCGGCC3′
3′CCGCGGCGAUCUGAACGG----GCAUAGUGCACCGGCCGG5′
```

bL

FIGURE 2. RNA hybrids under study. **A: P**otato **S**pindle **T**uber **V**iroi**d** (359 nt) in its native rodlike conformation. Different domains are abbreviated as follows: T_L, T_R, left and right terminal domain; Var, variable domain; CCR, central conserved region; VM, virulence-modulating region (see Keese & Symons, 1985). **B:** RNA duplexes representing the VM regions of the six strains studied [Mild, Intermediate, M1 in two conformations (cf. Text), Severe, Lethal, RG1]. The viroid sequence is numbered in Intermediate according to the nomenclature of Gross et al. (1978) and flanked on both sides by GC-"clamps" of 8 bp (in italics). Sequence differences for the other strains are in bold and underlined and are noted for each variant. Compared to Intermediate, Mild and Severe contain an additional difference outside of the VM region ($AA_{120-121} \rightarrow U$), which is not in the scope of this analysis. The RNA hybrids with a centrally located internal loop (iLA) or bulge loop (bL) served as controls to distinguish rigid bending from isotropic flexibility. The length standards of 36 and 39 bp dsRNA resulted from the annealing of complementary transcripts to the upper strands of the Mild VM region and the iLA duplex, respectively. Another dsRNA fragment of 43 bp was annealed from complementary transcripts with a random sequence (not shown).

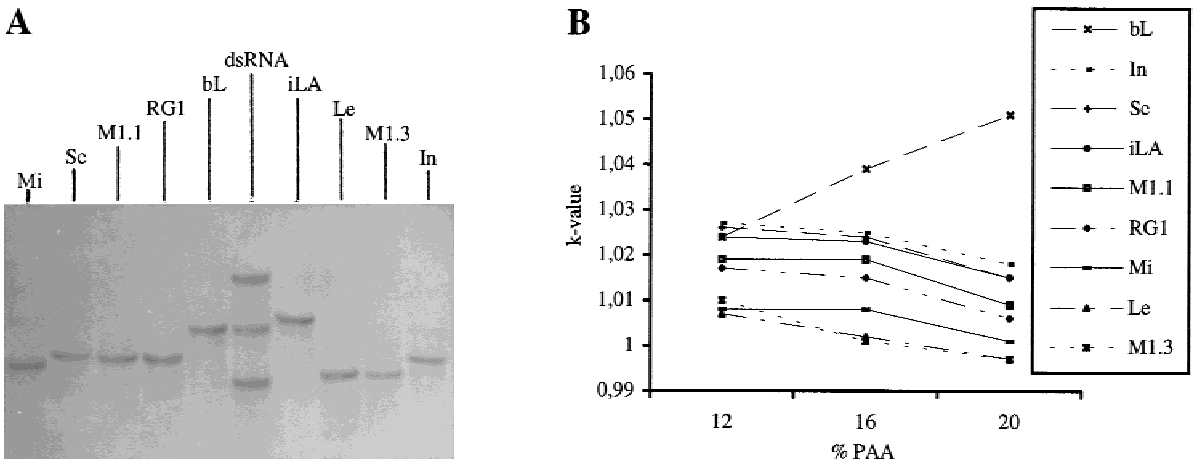

FIGURE 3. Gelelectrophoretic properties of VM regions and structure controls in the absence of Mg^{2+}. **A:** Native PAGE of VM region RNA duplexes in comparison to the three dsRNAs as length standards and to the bulge loop and internal loop containing fragments: Mi, Mild; Se, Severe; M1.1, thermodynamically most stable structure of the VM region of strain M1; RG1, RG1; bL, bulge loop; dsRNA, dsRNA of 36, 39 and 43 bp; iLA, internal loop; Le, Lethal; M1.3, suboptimal structure of the VM region of strain M1 (see text); In, Intermediate. Electrophoresis was done in a 20% polyacrylamide gel (acrylamide: bisacrylamide ratio 19:1) with 0.2× Na-TAE as gel and running buffer (no Mg^{2+}!). Temperature was held constant at 20 °C. Note the near normal mobility of the flexible internal loop compared with the pronounced retardation of the rigidly bent bulge loop. **B:** Plot of *k*-values for VM-region RNA duplexes and the bulge loop and internal loop containing fragments versus percent polyacrylamide in gels without Mg^{2+}. The *k*-value of an RNA duplex in a polyacrylamide gel is the apparent size (determined by comparison with the dsRNA fragments) divided by the true size. True sizes of the fragments are: In, M1.3, and Le: 36.5 bp; Mi, Se, M1.1, RG1, and bL: 37 bp; iLA: 39 bp, where bp means base pair equivalents in this case, because duplexes contain bulges and internal loops.

aly on polyacrylamide concentration in the gel. Except at the lowest gel concentration tested (12% PAA), the internal loop-containing duplex has a smaller *k*-value than its counterpart with the A_2-bulge loop. With rising PAA concentration, the *k*-value of the rigidly bent bL structure increases, whereas that of the flexible iLA structure decreases slightly. Addition of Mg^{2+} causes both to behave more like dsRNA of the same size, which is reflected in their reduced *k*-values (Fig. 4). This was not unexpected, because transient electric birefringence measurements showed that this ion reduces the size of the bulge-induced bends and confers

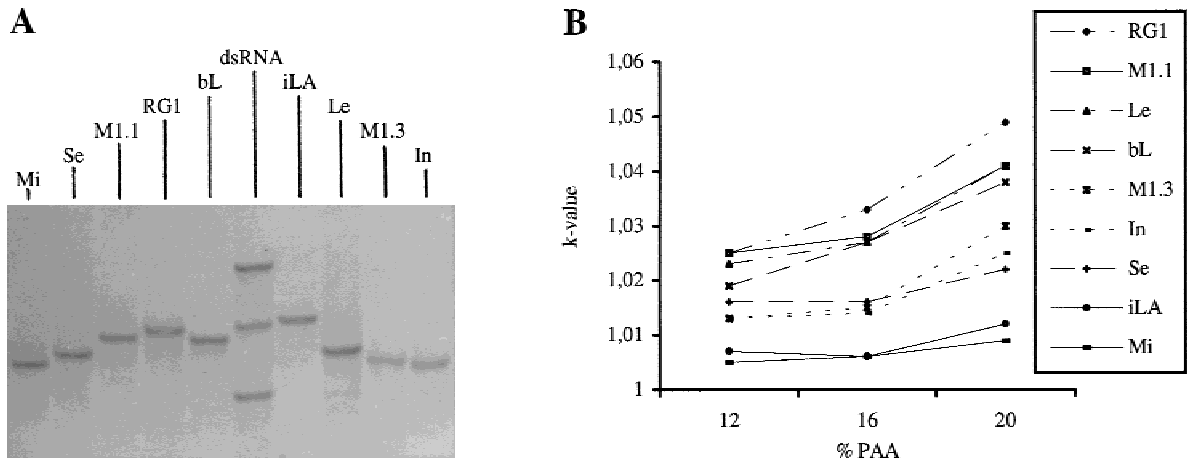

FIGURE 4. Gelelectrophoretic properties of VM regions and structure controls in the presence of Mg^{2+}. **A:** Native PAGE of the duplexes in the presence of 0.5 mM Mg^{2+}. Gel parameters are the same as in Figure 3, except for the buffer, which is 0.2× Na-TA, and the addition of 0.5 mM $MgSO_4$. Note especially the strong retardation of the very severe strains Lethal and RG1 compared to the experiment without Mg^{2+} shown in Figure 3A. **B:** Plot of *k*-values versus percent of polyacrylamide in the presence of 0.5 mM Mg^{2+}. The Mild VM region behaves nearly normally under these conditions, meaning that it is neither substantially bent nor flexible. Intermediate, M1.3, and Severe exhibit a modest, Lethal, M1.1, and especially RG1 a strong increase in their *k*-values with decreasing pore width of the gel. RG1 appears to be even more strongly kinked than duplex bL, which contains a centrally located A_2-bulge loop.

greater rigidity on internal loops, thus rendering both to show more duplex RNA-like behavior (Zacharias & Hagerman, 1995, 1996). Still, even in the presence of Mg^{2+}, the bent control has a greater *k*-value, which increases linearly with PAA concentration in the gel, whereas that of the flexible internal loop duplex is smaller and remains constant over the range of gel concentrations tested.

Flexibility of the VM region in the absence of Mg^{2+}

In the viroid context, several different base pairing schemes are possible for each VM region, whereas our constructs could only adopt a single conformation due to the presence of the stabilizing GC pairs at both ends. Therefore, they were designed to represent the thermodynamically most stable structure of the respective VM region, which was predicted by the program Linall (Schmitz & Steger, 1992). Mapping data available for the strains Intermediate, M1, and Lethal (Hammond, 1992 and R. Hammond, pers. comm.) strongly support these base pairing schemes shown in Figure 2. Only in the case of M1, a thermodynamically suboptimal structure—designated M1.3—was studied alongside; this was achieved easily by annealing the upper strand of Lethal to the lower one of Intermediate and was equivalent to leaving out G_{319} and thereby shifting the base pairing scheme to the suboptimal structure in the viroid context.

In the absence of Mg^{2+}, all of the VM regions exhibit a slight decrease of migration anomaly when the gel concentration is raised from 12 to 20% polyacrylamide (Fig. 3), thus reflecting the behavior of the flexible control with the centrally located internal loop. Moreover, the order of retardation is not at all in line with the differences in pathogenicity of the respective strains.

Correlation of VM region bending with pathogenicity in the presence of Mg^{2+}

Mg^{2+} was shown in many cases to be a mediator of physiologically active RNA structure (e.g., Laing et al., 1994). Therefore, we tested the gel electrophoretic behavior of the VM regions also in the presence of this cation. Addition of as little as 0.5 mM Mg^{2+} causes a rearrangement of the mobilities, with the order of migration anomalies now in line with the variants' pathogenicities (Fig. 4). When the gelelectrophoretic properties are compared to the behavior of the flexible and bent controls, it is possible to interpret the data at least semi-quantitatively in terms of bending of the VM region: whereas Mild, with a *k*-value of nearly 1, appears to be nearly as straight and rigid as a perfect RNA double helix of the same length, RG1 seems to be even more strongly kinked than the duplex with a centrally located A_2-bulge loop. Transient electric birefringence measurements revealed a bend of 31 ± 4° for this secondary structure element in the presence of 2 mM Mg^{2+} (Zacharias & Hagerman, 1995). Assigning this angle to the Lethal VM region because it behaves nearly identically to the A_2-bulge loop-control, one can estimate a bending angle for the VM regions of all strains by interpolating linearly the *k*-values at 20% PAA. The order of pathogenicity of the different strains is obvious from Figure 1. The pathogenicity of the PSTVd strains increases markedly from Mild to Intermediate, from M1 to Lethal and, finally, from Lethal to RG1, whereas M1 is only slightly more pathogenic than Intermediate, which holds true for the strain Severe as well (Schnölzer et al., 1985). In Figure 5, the bending angle, evaluated from the data in 0.5 mM Mg^{2+}, is plotted against the pathogenicity as determined by Owens et al. (1996). Most points agree with a linear relationship. The fact that strain M1 represents the only exception in this scheme in that its thermodynamically most stable structure (M1.1) is bent to the same extent as Lethal, calls into question whether in this case the suboptimal structure M1.3 dominates under cellular conditions, because this behaves as expected from the pathogenicity of this variant. The results shown in Figure 4 do not change upon raising the concentration of Mg^{2+} to 5 mM. The differences in the structures of the VM regions are noticeable even in the context of the whole PSTVd molecule, as could be shown by comparing the electrophoretic mobilities of the corresponding complete viroids, although these do not reflect the various degrees of pathogenicity (data not shown). This had already been observed by Singh et al. (1992) with still different PSTVd strains inducing mild to very severe symptoms.

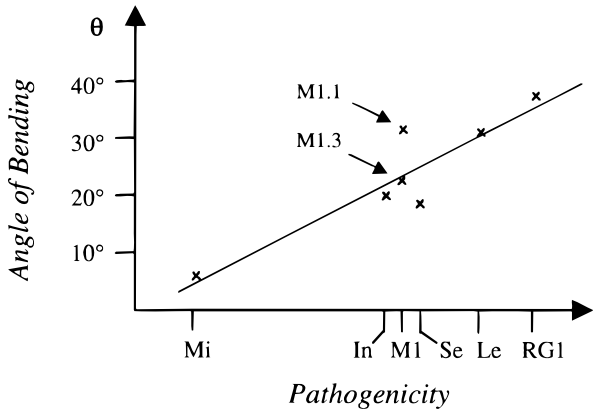

FIGURE 5. Estimated angle of VM-region bending versus pathogenicity. Lethal behaves as the A_2-bulge loop control in gels with magnesium, which exhibits a bend of approximately 30° under these conditions (Zacharias & Hagerman, 1996), whereas Mild shows a negligible migration anomaly and thus is supposed to be only very slightly bent. For strain M1, the suboptimal structure M1.3 is bent as expected from the pathogenicity of this strain, whereas its thermodynamically most stable structure M1.1 is surprisingly strongly kinked. The average heights of plants infected with the different PSTVd strains, as determined by Owens et al. (1996), served as an inverse measure of pathogenicity.

DISCUSSION

Structure of the VM region of PSTVd

The existence of viroid strains with remarkable differences in their pathogenicity had been realized long before their sequences became known (Diener, 1979). When the sequences of several PSTVd strains were determined, they showed only subtle differences in a restricted segment of the rod-like structure, the so-called VM region (Fig. 2). Early on, a model was proposed that not the sequence by itself was pathogenicity-determining, but the availability of the bases to a host component after the secondary structure of the restricted segment was dissociated, because calculations on four PSTVd strains suggested that the VM regions of more severe strains dissociate more easily (Schnölzer et al., 1985). However, the same model apparently did not apply to a series of CEVd strains (Visvader & Symons, 1985). When it was attempted to extend the model to nearly 20 different PSTVd strains, thermodynamic calculations and thermodynamic experiments were well in accordance, but could not be related to the symptom expression in a conclusive manner (Owens et al., 1996). Starting point of this work was a hypothesis that not the thermodynamic stability but the bending of the VM region was relevant for the primary molecular interaction.

We constructed RNA duplexes representing the VM regions of six different PSTVd strains. The open ends of this segment were stabilized by GC clamps on both sides. To probe their three dimensional structure, the mobilities in native PAGE were compared with those of perfect RNA duplexes of the same molecular weight. Such an approach has proven useful in testing for nucleic acid three-dimensional structure, for example to study the consequences of different loops on the flexibility or helix trajectory of unbranched nucleic acid structures (Bhattacharyya & Lilley, 1989; Zacharias & Hagerman, 1995, 1996). While bulge-loops introduce static bends whose size is dependent upon the number and nature of the unpaired bases, symmetric internal loops represent points of increased flexibility. This could be shown by phasing experiments, in which the distance between two such elements is varied by one to a few base pairs and hence their relative orientation changes with the periodicity of the helix (Rice & Crothers, 1989; Bhattacharyya et al., 1990; Tang & Draper, 1990; Kahn et al., 1994).

Reference RNAs of a size comparable to that of our VM-region hybrids allowed us to confirm that retardation in native PAGE increases for bent species when gel pore size is reduced, whereas it stays constant and is generally smaller for flexible structures, as found earlier with much longer duplexes (Bhattacharyya & Lilley, 1989; Kahn et al., 1994).

With this strategy, we found a striking correlation between bending of the VM region and pathogenicity of the respective strain (Fig. 5). The only exception to this correlation is strain M1, whose thermodynamically most stable structure is kinked more strongly than would be expected from its pathogenicity. The suboptimal structure M1.3, however, fits perfectly into the bending versus pathogenicity scheme, which might suggest that this structure is favored under cellular conditions.

The structural model presented here reflects the varying degrees of pathogenicity much better than the previous thermodynamic model. Besides M1, which did not fit into the thermodynamic scheme either, the VM regions of Mild and Intermediate were shown experimentally to have the same thermodynamic stabilities, as measured by the T_M value, as do Lethal and RG1, yet all these strains differ markedly with respect to their pathogenicities (Owens et al., 1996; Schmitz, 1989).

The fact that the correlation between structure of the VM region and pathogenicity exists only in the presence of Mg^{2+} and is clearly absent without Mg^{2+} demonstrates a marked structural rearrangement of the loops in the VM region upon the addition of Mg^{2+} ions and underlines the necessity to probe three-dimensional RNA structures in the presence of this physiologically relevant ion.

Models for pathogenic interaction of PSTVd

The earlier thermodynamic model for pathogenicity postulated an interaction with a nucleic acid of the host after the native secondary structure of PSTVd was dissociated. Contrary to this, we find a strong correlation between bending of the viroid's native structure and pathogenicity. In the native structure, however, no single-stranded stretches sufficiently long for a stable interaction with another nucleic acid are available. Thus, we regard host nucleic acids unlikely as partners and propose that the VM region's bending influences the affinity of the viroid to a protein of the host plant.

The physical principles of protein–RNA interactions are far from being completely understood, because, until now, only a few complexes have been determined with sufficient resolution. One of these is the U1A-protein bound to an internal loop in the 3′ UTR of its own mRNA (Allain et al., 1997). Here the RNA moiety is severely kinked, in the complex as well as in the unbound state (Grainger et al., 1997). Likewise, addition of Mg^{2+} leads to structural rearrangements in the isolated adenovirus VA_I–RNA that are similar to those observed when it binds to its target, the dsRNA-activated protein kinase PKR (Clarke & Mathews, 1995). Considering the entropy change upon complex formation, it is anyway most favorable if the RNA structure is ready for binding without additional structure formation, i.e., loss of entropy. Thus, even small differences in shape—as described in this work for the PSTVd strains—might have significant effects on complex stability.

Although the enzymes of the host's replication machinery are a priori candidates for the pathogenic interaction, a completely different enzyme, i.e., the dsRNA-activated protein kinase PKR, has been discussed for a long time as a putative target of the viroid RNA. Upon contact with dsRNA, it autophosphorylates itself and is then able to phosphorylate eukaryotic initiation factor 2 (eIF 2), leading to a rapid shutdown of translation initiation (for review, see Petryshyn et al., 1994). The process acts as an antiviral response of the organism, because transcription from the virus genome leads to the transient appearance of dsRNA, thereby activating PKR. Other functions of PKR, such as mediating apoptosis (Lee & Esteban, 1994; Srivastava et al., 1998) and cytokine-induced gene expression (Kumar et al., 1997), have been reported. Moreover, cellular RNAs have been identified that seem to specifically regulate PKR activity (Li et al., 1997; Chu et al., 1998).

The involvement of a plant homologue of PKR in viroid pathogenesis was first deduced from comparison of the phosphorylation state of proteins in healthy and viroid-infected tomato plants (Hiddinga et al., 1988). A 68-kDa species that crossreacted with antibodies directed against mammalian PKR was found to be specifically phosphorylated in the infected specimens. Antibody crossreaction and mutual recognition of the substrate eIF2 indicate a close homology of the plant and the mammalian PKR (Langland et al., 1995, 1996). Plant-PKR (pPKR) is likely to serve antiviral purposes, too, because its phosphorylation and thus activity is elevated in TMV-infected plants (Roth & He, 1994). The observation that a specific cellular inhibitor of PKR is upregulated when high translational activity is required shows that, in the plant also, PKR obviously serves several purposes (Langland et al., 1997). Both the plant and mammalian enzymes are ribosome-associated, but the latter was found also to be located in the nucleoli (Jiménez-Garcia et al., 1993). If this holds true for the plant PKR as well, a pathogenic interaction with PSTVd would be even more likely, because the circular viroids accumulate in this organelle (Schumacher et al., 1983; Harders et al., 1989). More direct experimental evidence for an interaction of PKR and PSTVd was first reported by Diener et al. (1993). They found a differential activation of the mammalian enzyme by different PSTVd strains, yet, even in the more effective cases, with only 1% of the dsRNA efficiency, which might be caused by the heterologous combination. Partially purified plant PKR binds to the left half of the rod-like PSTVd structure, which is the one containing the VM region (S. Zhang & T.O. Diener, communicated at the *Workshop on plant viroids and viroid like satellite RNAs from plants, animals and funghi*, Madrid, 1997). A similar interaction was found in the mammalian system; PKR binds to a discrete region of the viroid-like hepatitis-δ-RNA and is activated in vitro with approximately 20% of the efficiency of dsRNA (Robertson et al., 1996; Circle et al., 1997). This finding is surprising because (1) the enzyme is normally stringently dependent on perfect dsRNA and mismatches every eight base pairs lead to no detectable activation (Minks et al., 1979) and (2) the enzyme binds dsRNA in a non-sequence-specific manner. Thus, the bound segment in hepatitis-δ-RNA obviously mimics the PKR-binding features of dsRNA. The enzyme interacts with the minor groove of dsRNA and is dependent on contacts with 2′OH-groups on both strands (Bevilacqua & Cech, 1996). These findings suggest that it may well interact with RNAs that are not perfect double helices as long as these present the recognized groups in the correct context. Full activation of PKR requires stretches of 60–80 bp in length (Manche et al., 1992) and the protected region in δ-RNA represents 65 base pair analogues. Therefore, it seems probable that the VM region is not the only or even the primary part of PSTVd to which the plant PKR makes contacts, but merely functions as a sort of a hinge determining the relative orientation of adjacent parts relevant for the interaction.

MATERIALS AND METHODS

Preparation of RNA transcripts

DNA oligonucleotides for transcription of Mild, Intermediate, M1.3, Severe, and Lethal VM-region RNAs were synthesized on a 380 A DNA-synthesizer (Applied Biosystems) using β-cyanoethyl phosphoramidite chemistry, followed by deprotection and gel elution (see below) of the full-length products. Template strands for RG1 and M1.1 VM region RNAs and those for the dsRNA fragments and bL and iLA controls were purchased as HPLC-purified products from Interactiva. RNAs were transcribed in vitro from these synthetic DNA templates as described (Wyatt et al., 1991). Reaction volumes were 300 μL with a template concentration of 50 nM and 14 units T7-RNA-polymerase [purified as described by Wyatt et al. (1991)] per microliter. Incubation was at 37 °C for 3 h, with the addition of the same amount of polymerase after 90 min. Full-length transcripts were purified on 15% denaturing polyacrylamide gels and RNA was recovered by elution according to Krupp (1988) and ethanol precipitation.

Duplex formation of transcripts

Precipitated RNA was resuspended in annealing buffer (500 mM NaCl, 1 mM Na-Cacodylate, 0.1 mM EDTA, 4 M urea, pH 7.0) and complementary transcripts were electrophoresed as dilution series in denaturing PAGE for determination of concentration ratios. Equimolar amounts were then combined, heated to 75 °C, and cooled to room temperature overnight. RNA duplexes were precipitated, resuspended in dephosphorylation buffer (Boehringer, Mannheim) to a concentration of 0.1 pmol termini per microliter, and dephosphorylated for 2 h at 4 °C with 0.2 units alkaline phosphatase (Boehringer, Mannheim) per pmol termini.

RNA duplexes were dephosphorylated to avoid double bands in gels with magnesium. Reaction volumes were ex-

tracted with phenol/chloroform and nucleic acids were precipitated and resuspended in 0.2× Na-TAE (see below).

Gelelectrophoresis

Native PAGE was performed on a model SE 600 apparatus (Hoefer Scientific Instruments), where the gel is immersed in the anodic buffer reservoir whose temperature was held constant at 19 °C. Gel and running buffer was 0.2× Na-TAE (20 mM NaOAc, 8 mM Tris, 0.2 mM EDTA, pH 8.4) or 0.2× Na-TA (as Na-TAE but without EDTA) with $MgSO_4$ added to a concentration of 0.5 mM. Ratio of acrylamide to bisacrylamide in the gels was 19:1. The running buffer was recirculated and electrophoresis was performed at 27 V/cm for 2–13 h, depending on the percentage of the gel and presence or absence of Mg^{2+}.

Gels were fixed in 10% ethanol, 0.5% acetic acid for 10 min, stained with 10 mM $AgNO_3$ for 30 min, developed with 350 mM NaOH, 2 mM $NaBH_4$, 0.16% formaldehyde for 30 min, and neutralized in 90 mM $NaHCO_3$ for 10 min. Running distances of the probes were determined from enlarged photographs of the stained gels.

ACKNOWLEDGMENTS

We thank Dr. G. Steger for help with the thermodynamical calculations and many stimulating discussions and Dr. R. Hammond for kind provision of her mapping data. The work was supported by grants from the Deutsche Forschungsgemeinschaft and Fonds der Chemischen Industrie.

Received May 21, 1998; returned for revision June 26, 1998; revised manuscript received July 16, 1998

REFERENCES

Allain FHT, Howe PWA, Neuhaus D, Varani G. 1997. Structural basis of the RNA-binding specificity of human U1A protein. *EMBO J 16*:5764–5774.

Baumstark T, Schröder ARW, Riesner D. 1997. Viroid processing: Switch from cleavage to ligation is driven by a change from a tetraloop to a loop E conformation. *EMBO J 16*:599–610.

Bevilacqua PC, Cech TR. 1996. Minor-groove recognition of double-stranded RNA by the double-stranded RNA-binding domain from the RNA-activated protein kinase PKR. *Biochemistry 35*:9983–9994.

Bhattacharyya A, Lilley DMJ. 1989. The contrasting structures of mismatched DNA sequences containing looped-out bases (bulges) and multiple mismatches (bubbles). *Nucleic Acids Res 17*:6821–6840.

Bhattacharyya A, Murchie AIH, Lilley DMJ. 1990. RNA bulges and the helical periodicity of double-stranded RNA. *Nature 343*:484–487.

Branch AD, Robertson HD. 1984. A replication cycle for viroids and other small infectious RNAs. *Science 223*:450–455.

Chu WM, Ballard R, Carpick BW Williams BRG, Schmid CW. 1998. Potential Alu function: Regulation of the activity of double-stranded RNA-activated kinase PKR. *Mol Cell Biol 18*:58–68.

Circle DA, Neel OD, Robertson HD, Clarke PA, Mathews MB. 1997. Surprising specificity of PKR binding to delta agent genomic RNA. *RNA 3*:438–448.

Clarke PA, Mathews MB. 1995. Interactions between the double-stranded RNA binding motif and RNA: Definition of the binding site for the interferon-induced protein kinase DAI (PKR) on adenovirus VA RNA. *RNA 1*:7–20.

Diener TO. 1971. Potato Spindle Tuber "Virus", IV. A replicating, low molecular weight RNA. *Virology 45*:411–428.

Diener TO. 1979. *Viroids and viroid diseases*. New York: Wiley.

Diener TO, ed. 1987. *The viroids*. New York: Plenum Publishing Corporation.

Diener TO, Hammond RW, Black T, Katze MG. 1993. Mechanism of viroid pathogenesis: Differential activation of the interferon-induced, double-stranded RNA-activated, M_r 68000 protein kinase by viroid strains of varying pathogenicity. *Biochimie 75*:533–538.

Diener TO, Raymer WB. 1967. Potato Spindle Tuber Virus: A plant virus with properties of a free nucleic acid. *Science 158*:378–381.

Grainger RJ, Murchie AIH, Norman DG, Lilley DMJ. 1997. Severe axial bending of RNA induced by the U1A binding element present in the 3′ untranslated region of the U1A mRNA. *J Mol Biol 273*:84–92.

Gross HJ, Domdey H, Lossow C, Jank P, Raba M, Alberty H, Sänger HL. 1978. Nucleotide sequence and secondary structure of potato spindle tuber viroid. *Nature 273*:203–208.

Gruner R, Fels A, Qu F, Zimmat R, Steger G, Riesner D. 1995. Interdependence of pathogenicity and replicability with potato spindle tuber viroid. *Virology 209*:60–69.

Hammond R. 1992. Analysis of the virulence modulating region of Potato Spindle Tuber Viroid (PSTVd) by site-directed mutagenesis. *Virology 187*:654–662.

Harders J, Lukács N, Robert-Nicoud M, Jovin TM, Riesner D. 1989. Imaging of viroids in nuclei from tomato leaf tissue by in situ hybridization and confocal laser scanning microscopy. *EMBO J 8*:3941–3949.

Hiddinga HJ, Crum CJ, Hu J, Roth DA. 1988. Viroid-induced phosphorylation of a host protein related to a dsRNA-dependent protein kinase. *Science 241*:451–453.

Jiménez-Garcia LF, Green SR, Mathews MB, Spector DL. 1993. Organization of the double-stranded RNA-activated protein kinase DAI and virus-associated VA RNA_1 in adenovirus-2-infected HeLa cells. *J Cell Sci 106*:11–22.

Kahn JD, Yun E, Crothers DM. 1994. Detection of localized DNA flexibility. *Nature 368*:163–166.

Keese P, Symons RH. 1985. Domains in viroids: Evidence of intermolecular RNA rearrangements and their contribution to viroid evolution. *Proc Natl Acad Sci USA 82*:4582–4586.

Krupp G. 1988. RNA synthesis: Strategies for the use of bacteriophage RNA polymerases. *Gene 72*:75–89.

Kumar A, Yang YL, Flati V, Der S, Kadereit S, Deb A, Haque J, Reis L, Weissmann C, Williams BRG. 1997. Deficient cytokine signaling in mouse embryo fibroblasts with a targeted deletion in the PKR gene: Role of IRF-1 and NF-κB. *EMBO J 16*:406–416.

Laing LG, Gluick TC, Draper DE. 1994. Stabilization of RNA structure by Mg ions. Specific and non-specific effects. *J Mol Biol 237*:577–587.

Langland JO, Jin S, Jacobs BL, Roth DA. 1995. Identification of a plant-encoded analog of PKR, the mammalian double-stranded RNA-dependent protein kinase. *Plant Physiol 108*:1259–1267.

Langland JO, Langland LA, Browning KS, Roth DA. 1996. Phosphorylation of plant eukaryotic initiation factor-2 by the plant-encoded double-stranded RNA-dependent protein kinase, pPKR, and inhibition of protein synthesis in vitro. *J Biol Chem 271*:4539–4544.

Langland JO, Langland L, Zeman C, Saha D, Roth DA. 1997. Developmental regulation of a plant encoded inhibitor of eukaryotic initiation factor 2α phosphorylation. *Plant J 12*:393–400.

Lee SB, Esteban M. 1994. The interferon-induced double-stranded RNA-activated protein kinase induces apoptosis. *Virology 199*:491–496.

Li JH, Yu ZP, Lomiany DJ, Petryshyn RA. 1997. Characterization of a cellular RNA that activates PKR in 3T3 F442 A cells. *Inter J Oncol 11*:685–695.

Manche L, Green SR, Schmedt C, Mathews MB. 1992. Interactions between double-stranded RNA regulators and the protein kinase DAI. *Mol Cell Biol 12*:5238–5248.

Minks MA, West DK, Benvin S, Baglioni C. 1979. Structural requirements of double-stranded RNA for the activation of 2′,5′-oligo(A) polymerase and protein kinase of interferon-treated HeLa cells. *J Biol Chem 254*:10180–10183.

Owens RA, Steger G, Hu Y, Fels A, Hammond RW, Riesner D. 1996. RNA structural features responsible for potato spindle tuber viroid pathogenicity. *Virology 222*:144–158.

Petryshyn RA, Li J, Judware R. 1994. Activation of the dsRNA-dependent kinase. *Progr Mol Subcell Biol 14*:1–14.

Rice JA, Crothers DM. 1989. DNA bending by the bulge defect. *Biochemistry 28*:4512–4516.
Riesner D, Gross HJ. 1985. Viroids. *Annu Rev Biochem 54*:531–564.
Robertson HD, Manche L, Mathews MB. 1996. Paradoxical interactions between human delta hepatitis agent RNA and the cellular protein kinase PKR. *J Virol 70*:5611–5617.
Roth DA, He X. 1994. Viral-dependent phosphorylation of a dsRNA-dependent kinase. *Prog Mol Subcell Biol 14*:28–46.
Schindler IM, Mühlbach HP. 1992. Involvement of nuclear DNA-dependent RNA polymerases in potato spindle tuber viroid replication: A reevaluation. *Plant Science 84*:221–229.
Schmitz M. 1989. *Experimentelle und theoretische Untersuchungen an partiell basengepaarten Bereichen in Nukleinsäuren* [thesis]. Heinrich-Heine-Universität Düsseldorf.
Schmitz M, Steger G. 1992. Base-pair probability profiles of RNA secondary structures. *Comp Appl Biosci 8*:389–399.
Schnölzer M, Haas B, Ramm K, Hofmann H, Sänger HL. 1985. Correlation between structure and pathogenicity of potato spindle tuber viroid (PSTV). *EMBO J 4*:2181–2190.
Schumacher J, Sänger HL, Riesner D. 1983. Subcellular localization of viroids in highly purified nuclei from tomato leaf tissue. *EMBO J 2*:1549–1555.
Semancik JS, ed. 1987. *Viroids and viroid-like pathogens*. Boca Raton, Florida: CRC Press.
Singh RP, Boucher A, Haas B, Sänger HL. 1991. Differential migration during polyacrylamide gel electrophoresis suggests conformational differences among strains of potato spindle tuber viroid. *Can J Plant Pathol 13*:202–211.
Srivastava SP, Kumar KU, Kaufman RJ. 1998. Phosphorylation of eukaryotic translation factor 2 mediates apoptosis in response to activation of the double-stranded RNA-dependent protein kinase. *J Biol Chem 273*:2416–2423.
Symons RH, ed. 1990. Viroids and related pathogenic RNAs. *Semin Virol 1*.
Tang RS, Draper DE. 1990. Bulge loops used to measure the helical twist of RNA in solution. *Biochemistry 29*:5232–5236.
Visvader JA, Symons RH. 1985. Eleven new sequence variants of citrus exocortis viroid and correlation of sequence with pathogenicity. *Nucleic Acids Res 13*:2907–2920.
Wyatt JR, Chastain M, Puglisi JD. 1991. Synthesis and purification of large amounts of RNA oligonucleotides. *BioTechniques 11*:764–769.
Zacharias M, Hagerman PJ. 1995. Bulge-induced bends in RNA: Quantification by transient electric birefringence. *J Mol Biol 247*:486–500.
Zacharias M, Hagerman PJ. 1996. The influence of symmetric internal loops on the flexibility of RNA. *J Mol Biol 257*:276–289.